Lithuanian Journal of Physics
Vol. **64**, No. 2, pp. 73–81 (2024)

ISSN 1648-8504 eISSN 2424-3647
DOI: https://doi.org/10.3952/physics.2024.64.2.1

SECOND-ORDER RAYLEIGH–SCHRÖDINGER PERTURBATION THEORY FOR THE GRASP2018 PACKAGE: CORE CORRELATIONS*

G. Gaigalas, P. Rynkun, and L. Kitovienė

Institute of Theoretical Physics and Astronomy, Vilnius University, Saulėtekio 3, 10257 Vilnius, Lithuania
Email: gediminas.gaigalas@tfai.vu.lt; pavel.rynkun@tfai.vu.lt; laima.radziute@tfai.vu.lt

Received 19 February 2024; accepted 27 March 2024

The paper presents a further development of the method presented in G. Gaigalas, P. Rynkun, and L. Kitovienė, Second-order Rayleigh–Schrödinger perturbation theory for the GRASP2018 package: core–valence correlations, Lith. J. Phys. 64(1), 20–39 (2024) (https://doi.org/10.3952/physics.2024.64.1.3), based on a combination of the relativistic configuration interaction method and on the stationary second-order Rayleigh–Schrödinger many-body perturbation theory in an irreducible tensorial form. In this extension, the perturbation theory accounts for both electron core–valence and core correlations when an atom or ion has any number of valence electrons, while the relativistic configuration interaction accounts for the rest of correlations. This allows a significant reduction of the space of the configuration state functions for complex atoms and ions. We also demonstrate how this method works for the energy structure calculation of Fe XV ion.

Keywords: configuration interaction, spin-angular integration, perturbation theory, tensorial algebra, core–valence correlations, core correlations

1. Introduction

A major challenge in atomic structure calculations is the accurate description of electron correlations. Many powerful theoretical methods, such as different versions of many-body perturbation theory (MBPT) [1, 2], the configuration interaction method (CI) [3], the relativistic configuration interaction (RCI) [4], the random phase approximation with exchange (RPAE) [5, 6], the multiconfiguration Hartree–Fock method (MCHF) [7] or the multiconfiguration Dirac–Hartree–Fock (MCDHF) method [8], have been developed to account for correlation effects. These methods have their own disadvantages in obtaining highly accurate atomic data. For example, the inclusion of correlation effects in the MCHF, MCDHF, or CI methods rapidly increases the expansion of atomic state function (ASF), especially for complex atoms. Perturbation theory (PT) has practical and theoretical difficulties for degenerate states, especially in selecting the model space [1]. The structure of terms of the PT series often leads to one- and two-particle operators, which almost in all versions of many-body perturbation theory are not in an irreducible tensorial form and cannot use the advantage of Racah algebra [9, 10].

Probably the most efficient and consistent way to account for correlation and relativistic effects simultaneously is to combine RCI and relativistic many-body perturbation theory methods [11, 12]. This is particularly relevant for complex many-electron atoms with open f-shells, such as lanthanides and actinides, when calculating energy spectra and other properties.

A combination of the relativistic configuration interaction method and the stationary second-order Rayleigh–Schrödinger many-body perturbation theory in an irreducible tensorial form [13] has been already developed and implemented in the GRASP2018 package [14] to account for the core–valence correlations. In this paper, we

---

* Dedicated to the memory of professor **Adolfas Jucys** (1904–1974), pioneer of contemporary theoretical physics in Lithuania, initiator of the 'Lithuanian Physics Collection', on the occasion of his birth and death anniversaries.

present the extension of this method (see Section 2) when core correlations are added, and show how to use it in real applications (see Section 3).

2. Combination of the RCI method with the stationary second-order Rayleigh–Schrödinger many-body perturbation theory

In regular GRASP [14, 15] calculations, to obtain radial orbitals, the main correlations are included in the MCDHF calculations. This is followed by RCI calculations to add other important correlations via the configuration state functions (CSFs). To include valence (V) and valence–valence (VV) correlations, the space is extended by CSFs, in which one or two electrons are excited from valence orbitals to virtual orbitals. Other types of correlations, such as core–valence (CV) and core (C) correlations, are added in the same manner.

In this paper, we present a combination of the RCI method and the stationary second-order Rayleigh–Schrödinger many-body perturbation theory in an irreducible tensorial form, RCI (RSMBPT), where CV and C correlations are included according to the RSMBPT. The inclusion of CV correlations using the RCI (RSMBPT) method has already been developed and it can be found in Ref. [13] with the expressions and its implementation in the GRASP package. This contribution coming from the CV correlations of the configurations K' to $E(K\chi J)$ in the second order of perturbation theory is expressed as Eq. (22) of Ref. [13],

$$
\begin{aligned}
&\Delta E_{\mathrm{PT(CV)}} = \\
&= \Delta\mathcal{E}_0(KJ) + \\
&+\sum_{n\ell j}\sum_{k>0} \tilde{f}_k(\ell j^w, K\chi J)\Delta\mathcal{F}^k(n\ell j, n\ell j) + \\
&+\sum_{n\ell j}\sum_{n'\ell' j'>n\ell j}\Bigg\{\sum_{k>0}\tilde{f}_k(\ell j^w\ \ell' j'^{w'}, K\chi J)\times \\
&\qquad\qquad \times\Delta\mathcal{F}^k(n\ell j, n'\ell' j') + \\
&+\sum_k \tilde{g}_k(\ell j^w\ \ell' j'^{w'}, K\chi J)\Delta\mathcal{G}^k(n\ell j, n'\ell' j') + \\
&+\sum_k \tilde{v}_k(\ell j^w\ \ell' j'^{w'}, \ell j^{w-2}\ \ell' j'^{w'+2}, K\chi J\ K'\chi' J')\times \\
&\qquad\qquad \times\Delta\mathcal{R}^k(n\ell j n\ell j, n'\ell' j' n'\ell' j')\Bigg\}. \qquad (1)
\end{aligned}
$$

Here we extend the combination of the RCI method with RSMBPT to include the core correlations via perturbation theory, which has already been used for CV correlations in Ref. [13]. This allows even greater reduction of the CSF space for the RCI method. The Feynman diagrams corresponding to the following type of core correlation are shown in Fig. 1, where all lines with a double arrow of diagrams are renamed m, i.e. $m' \equiv m$:

$$(n_a\ell_a) j_a^{2ja+1} (n_m\ell_m) j_m^{wm} \to (n_a\ell_a) j_a^{2ja} (n_m\ell_m) j_m^{wm} (n_r\ell_r) j_r. \qquad (2)$$

These are the same four two-particle Feynman diagrams which partly describe CV correlations (see Ref. [13]). The detailed explanations and expressions in an irreducible tensorial form of the diagrams are presented in Ref. [13].

It should also be mentioned that the method proposed in the paper does not allow the following type of core and core–valence correlations to be included via RSMBPT:

$$(n_a\ell_a) j_a^{2ja+1} (n_m\ell_m) j_m^{wm} \to (n_a\ell_a) j_a^{2ja} (n_m\ell_m) j_m^{wm+1}, \qquad (3)$$

$$
\begin{aligned}
&(n_a\ell_a) j_a^{2ja+1} (n_m\ell_m) j_m^{wm} (n_n\ell_n) j_n^{wn} \to \\
&\to (n_a\ell_a) j_a^{2ja} (n_m\ell_m) j_m^{wm-1} (n_n\ell_n) j_n^{wn+2}. \qquad (4)
\end{aligned}
$$

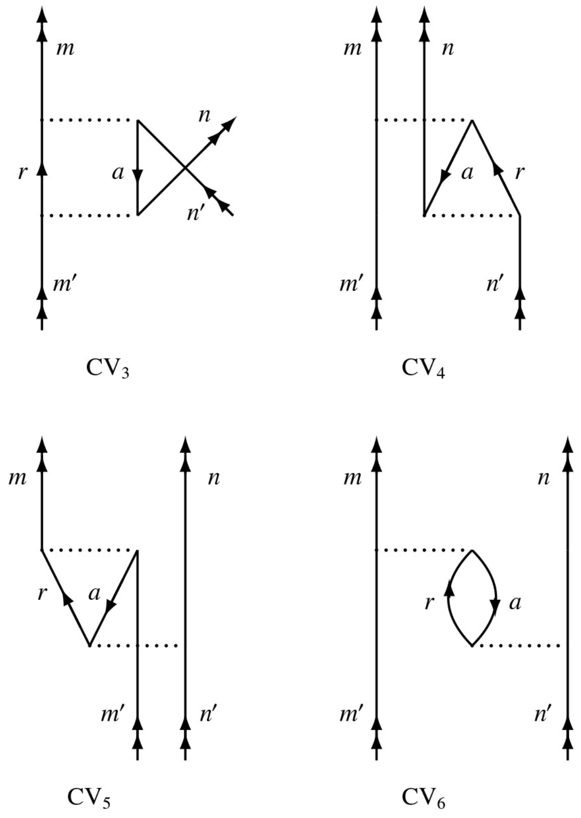

CV$_3$ CV$_4$

CV$_5$ CV$_6$

Fig. 1. The CV Feynman diagrams of the second-order effective Hamiltonian for core correlations $(n_a\ell_a) j_a^{2ja+1} (n_m\ell_m) j_m^{wm} \to (n_a\ell_a) j_a^{2ja} (n_m\ell_m) j_m^{wm} (n_r\ell_r) j_r$.

This is related to the fact that these C (Eq. (2)) and CV (Eq. (3)) correlations described via Feynman diagrams depend on the potential of the radial orbitals found. This makes the implementation of this type of correlations impossible to be included in the RSMBPT method for any potential of MCDHF equations. Therefore, these correlations should be included in the RCI calculations in a regular way.

According to Ref. [11], the energy contribution of the admixed configurations from C correlations (Eq. (2)) can be added to a regular energy of the term χJ of the configuration K and can be expressed as the energy $E_0(KJ)$, which does not depend on the term, and the sum of the product of Slater integrals and spin-angular coefficients:

$$\begin{aligned} E(K\chi J) &= E_0(KJ) + \Delta\mathcal{E}_0(KJ) + \\ &+ \sum_{n\ell j}\sum_{k>0} \tilde{f}_k(\ell j^w, K\chi J)\big[\mathcal{F}^k(n\ell j, n\ell j) + \\ &+ \Delta\mathcal{F}^k(n\ell j, n\ell j)\big]. \end{aligned} \quad (5)$$

The contribution of the C correlations in the second-order of perturbation theory according to Eq. (5) can be expressed as

$$\begin{aligned} \Delta E_{\mathrm{PT(C)}} &= \Delta\mathcal{E}_0(KJ) + \\ &+ \sum_{n\ell j}\sum_{k>0} \tilde{f}_k(\ell j^w, K\chi J)\Delta\mathcal{F}^k(n\ell j, n\ell j). \end{aligned} \quad (6)$$

$\Delta\varepsilon_0(KJ)$ (see Table 1), the contribution of C correlations in the second-order of perturbation theory deriving from the total energy $E_0(KJ)$, can be expressed through $\mathcal{A}$, $\mathcal{D}$ and $\mathcal{C}$ coefficients, which have the following expressions:

$$\begin{aligned} \mathcal{A}(x, ij, i'j') &= \\ &= \sum_{k,k'} \begin{Bmatrix} k & k' & x \\ j_i & j_i & j_{i'} \end{Bmatrix} \begin{Bmatrix} k & k' & x \\ j_{j'} & j_{j'} & j_j \end{Bmatrix} \mathcal{P}(kk', ij, i'j'), \end{aligned} \quad (7)$$

$$\begin{aligned} \mathcal{D}(ij, i'j') &= \mathcal{P}(00, ij, i'j') + \\ &+ \frac{2}{\sqrt{[j_i, j_j]}} \sum_k (-1)^{j_i + j_j + k} Q(0k, ij, i'j'), \end{aligned} \quad (8)$$

$$\mathcal{C}(k, ij, i'j') = \sum_{k'} \begin{Bmatrix} k & j_i & j_{i'} \\ k' & j_j & j_{j'} \end{Bmatrix} Q(kk', ij, i'j'), \quad (9)$$

$$\mathcal{P}\,(kk', ij, i'j') = \mathcal{R}^k\,(ij, i'j')\,\mathcal{R}^{k'}\,(i'j', ij)\,\mathcal{O}\,(K', K), \quad (10)$$

$$Q\,(kk', ij, i'j') = \mathcal{R}^k\,(ij, i'j')\,\mathcal{R}^{k'}\,(i'j', ji)\,\mathcal{O}\,(K', K). \quad (11)$$

We would like to emphasize that the energy denominator is defined differently (with the opposite sign) than in the expressions of Feynman diagrams (see, for example, Ref. [13], Fig. 3, Eqs. (10) and (11)):

$$\mathcal{O}(K', K) = \frac{1}{\bar{E}(K') - \bar{E}(K)}. \quad (12)$$

The $\mathcal{R}^k$ is the generalized integral of the electrostatic interaction between electrons in Table 1:

$$\begin{aligned} \mathcal{R}^k(ij, i'j') &= \{[1 + \delta(i, j)][1 + \delta(i', j')]\}^{-1/2} \times \\ &\times R^k(n_i j_i n_j j_j, n_{i'} j_{i'} n_{j'} j_{j'}) \times \\ &\times \langle \ell_i j_i \| C^{(k)} \| \ell_{i'} j_{i'} \rangle \langle \ell_j j_j \| C^{(k)} \| \ell_{j'} j_{j'} \rangle. \end{aligned} \quad (13)$$

Here $R^k(n_i j_i\, n_j j_j, n_{i'} j_{i'}\, n_{j'} j_{j'})$ is the radial integral.

Table 1. Expressions for the core corrections to the energy in Eq. (5), not depending on the term.

$\Delta\mathcal{E}_0$ corrections
$\overbrace{(n_a\ell_a)j_a^{2j_a+1}}^{\text{core subshells}}\ \overbrace{(n_m\ell_m)j_m^{w_m}}^{\text{valence subshells}} \rightarrow \overbrace{(n_a\ell_a)j_a^{2j_a}}^{\text{core subshells}}\ \overbrace{(n_m\ell_m)j_m^{w_m}}^{\text{valence subshells}}\ \overbrace{(n_r\ell_r)j_r}^{\text{virtual subshells}}$
$\frac{w_m}{[j_m]}\left\{\underbrace{(w_m - 1 - [j_m])\mathcal{A}(0, ma, rm)}_{\text{from CV}_3\text{ Feynman diagram}} \underbrace{-(w_m - 1)\ \mathcal{D}(ma, mr)\delta(j_r, j_a)}_{\text{from CV}_4\text{, CV}_5\text{ and CV}_6\text{ Feynman diagrams}}\right\}$
$+\frac{w_m(-1)^{j_a + j_r}}{[j_m]}\left\{\underbrace{2\sum_k \mathcal{C}(k, ma, mr)}_{\text{from CV}_4\text{ and CV}_5\text{, Feynman diagrams}} \underbrace{+\sum_k \frac{1}{[k]}\mathcal{P}(kk, ma, mr)}_{\text{from CV}_6\text{, Feynman diagram}}\right\}$

Table 2. Expressions for the Slater integrals $\Delta\mathcal{F}^k\,(m, m)$ (see Eq. (5)) corresponding to the core $(n_a\ell_a)\, j_a^{2j_a+1}\,(n_m\ell_m)\, j_m^{w_m} \rightarrow (n_a\ell_a)\, j_a^{2j_a}\,(n_m\ell_m)\, j_m^{w_m}\,(n_r\ell_r)\, j_r$ correlations.

Corrections	Slater integral	k values
$\underbrace{2[k]\,\mathcal{Y}(1,k,ma,rm,mm)}_{\text{from CV}_3\text{ Feynman diagram}} + (-1)^{j_a+j_r+k}\left\{\underbrace{4\,\mathcal{Z}(1,k,ma,mr,mm)}_{\text{from CV}_4\text{ and CV}_5\text{ Feynman diagrams}} + \underbrace{\frac{2}{[k]}\,\mathcal{P}(kk,ma,mr)}_{\text{from CV}_6\text{ Feynman diagram}}\right\}$	$\Delta\mathcal{F}^k(m, m)$	$k > 0$

The contribution of C correlations in the second-order of perturbation theory arriving at $\mathcal{F}^k\,(n\ell j, n\ell j)$ and $\Delta\mathcal{F}^k\,(n\ell j, n\ell j)$ (see Table 2) can be expressed through $\mathcal{Y}$ and $\mathcal{Z}$ coefficients. These have the following expressions:

$$\mathcal{Y}(1, x, ij, i'j', i''j'') = \\ = \sum_{k,k'} (-1)^{k+k'+x} \begin{Bmatrix} k & k' & x \\ j_{i''} & j_i & j_{i'} \end{Bmatrix} \begin{Bmatrix} k & k' & x \\ j_{j''} & j_{j'} & j_j \end{Bmatrix} \times \\ \times\, \mathcal{T}(1, kk', ij, i'j', i''j''), \quad (14)$$

$$\mathcal{T}(1, kk', ij, i'j', i''j'') = \\ = \mathcal{R}^k\,(ij, i'j')\, \mathcal{R}^{k'}\,(i'j'', i''j)\; \mathcal{O}\,(K', K), \quad (15)$$

$$\mathcal{Z}(1, k, ij, i'j', i''j'') = \\ = \sum_{k'} \begin{Bmatrix} k & j_{i''} & j_{j''} \\ k' & j_j & j_{j'} \end{Bmatrix} \mathcal{U}\,(1, kk', ij, i'j', i''j''), \quad (16)$$

$$\mathcal{U}(1, kk', ij, i'j', i''j'') = \\ = \mathcal{R}^k\,(ij, i'j')\, \mathcal{R}^{k'}\,(j''j', ji'')\; \mathcal{O}\,(K', K). \quad (17)$$

3. Calculation of core–valence and core correlations with a new approach

As described in the above section, the method based on the Rayleigh–Schrödinger perturbation theory in an irreducible tensorial form [13] is extended to include C correlations in the computations. This section aims to present the results when the CV and C correlations are included in a regular way and using the stationary second-order Rayleigh–Schrödinger many-body perturbation theory in an irreducible tensorial form. For this purpose, we computed the energy levels of the 3s^2, 3p^2, 3s3d, 3d^2, 3p3d and 3s3p configurations of Fe XV. Below the computational procedure and results from the regular GRASP2018 and RCI (RSMBPT) computations are presented.

3.1. Computational scheme

An initial MCDHF calculation for the even and odd states of 3s^2, 3p^2, 3s3d, 3d^2, 3p3d and 3s3p configurations was done in the extended optimal level (EOL) scheme [16]. The initial calculation was followed by separate calculations in the EOL scheme for the even and odd parity states. The space of CSFs, referred to as the active space (AS), building the atomic state function (ASFs), was obtained using the multireference-single-double (MR-SD) method [4]. The MR set consists of the 3s^2, 3p^2, 3s3d, 3d^2 even and 3p3d, 3s3p odd configurations. The orbital spaces (OS), to which single and double (SD) substitutions from the configurations in the MR were allowed, are OS$_1$ = {4s, 4p_, 4p, 4d_, 4d, 4f_, 4f}, ..., OS$_5$ = {8s, 8p_, 8p, 8d_, 8d, 8f_, 8f, 8g_, 8g, 8i_, 8i}. SD substitutions were allowed from the 3s, 3p_, 3p, 3d_, 3d orbitals, and S substitutions were allowed only from the 2s or 2p_ and 2p core orbital. Only CSFs that have non-zero matrix elements with the CSFs belonging to the configurations in the MR were retained. No substitutions were allowed from the 1s^2 core, which defines an inactive closed core. Based on the orbitals from the MCDHF calculations, RCI calculations were further performed, including the Breit interaction and leading quantum electrodynamic (QED) effects – the vacuum polarization and self-energy corrections. Regular RCI calculations are marked as CV+C RCI.

The results of the calculation when the CV and C correlations are included according to the RSMBPT method are marked as CV+C RCI

(RSMBPT). In this case, we use a program to determine the contribution of each *K*′ configuration of the CV and C correlations for CSF, for which energy needs to be calculated according to Rayleigh–Schrödinger perturbation theory in an irreducible tensorial form according to Eqs. (1) and (6). The program calculates the total contribution of the CV and C correlations and the contribution of each *K*′ configuration of these correlations for the computed levels. *K*′ configurations are sorted in a descending order according to the impact of the CV and C correlations for each level. Further, we select *K*′ configurations by the CV and C correlations impact with the specified fraction (expressed in the percentage) of the total CV and C contribution, and perform RCI computations including them. The calculations using the RSMBPT method were carried out using different amounts of CV and C correlations: 95, 99, 99.5, 99.95 and 100%. In the RSMBPT method, the CSF space is divided into three sets: *F*, *F*′ and *G* (see Ref. [13] for details). Thus in RSMBPT computations, the 1s is also defined as an inactive core subshell, 2s, 2p_ and 2p subshells are defined as active core subshells (that correspond to the *F* set), 3s, 3p_, 3p, 3d_ and 3d as valence subshells (that correspond to the *F*′ set), and subshells belonging to OS_1, ..., OS_5 as virtual ones (that correspond to the *G* set). This distribution of space is consistent with regular GRASP calculations and allows the use of a combination of RCI and RSMBPT methods. It should be noted that the program gives the contribution of the CV and C correlations of *K*′ configuration with the value greater than 1.0E-11, the rest contributions are neglected. Therefore a number of CSFs, when 100% of CV and C correlations are included, is smaller than in the regular CV+C RCI calculations. The C (Eq. (3)) and CV (Eq. (4)) correlations (mentioned above in Section 2), which were not included with the RSMBPT method, were added to the RCI calculations in a regular way, together with the valence and valence–valence correlations.

3.2. Results

Table 3 presents the total energies from regular GRASP2018 calculations (CV+C RCI) for 35 computed states and differences of energies using the CV+C RCI (RSMBPT) method with the CV+C RCI results, $\Delta E_{\text{(CV+C RCI (RSMBPT))-(CV+C RCI)}}$. In the last line of the table, the number of CSFs (N_{CSFs}) from each calculation is given. It is seen from the table that the results obtained with the RSMBPT method converge to regular RCI results (CV+C RCI) by including step by step the most important *K*′ configurations of CV and C correlations. The calculations using the RSMBPT method are carried out in five steps, including 95, 99, 99.5, 99.95 and 100% of CV and C correlations. In case when all contributions of the CV and C correlations (column 100%) given by the program are included in the computations, the CV+C RCI (RSMBPT) reproduce the results of regular RCI computations. The negligible difference (to 4.0E-06 a.u.) in the 100% column could be due to omitted CV and C correlations with a very small contribution (1.0E-11), as it was mentioned above.

In Table 4, the energy levels from the regular GRASP2018 calculations CV+C RCI and from the calculations using the RSMBPT method CV+C RCI (RSMBPT) are compared. The energy levels from the Atomic Spectra Database (ASD) of the National Institute of Standards and Technology (NIST; Ref. [17]) are also given. As shown in Table 4, by adding the most important *K*′ configurations of CV and C correlations step by step (as in Table 3), the results smoothly converge to the CV+C RCI results. In case when 99% of CV and C correlations are included in the computations, the results are close to those of CV+C RCI. The difference between the results of these calculations is only few tens of cm^{-1} (which is a hundredth of a percent of our calculated energy levels), and in this case, the number of CSFs decreases twice compared to the space in the CV+C RCI computations. By increasing the percentage of the CV and C correlations included in the CV+C RCI (RSMBPT) calculations, the difference between the results of CV+C RCI (RSMBPT) and CV+C RCI decreases. The results in the 100% column are in excellent agreement with the regular GRASP2018 calculations. A difference of up to 1 cm^{-1} could be due to the omission of the CV and C correlations with contribution less than 1.0E-11 (as mentioned above, the program excludes configurations with a very small contribution).

Thus, it can be seen that the RCI (RSMBPT) method, when CV and C correlations are included, produces results that match the regular ones. By

Table 3. Total energies (in a.u.) from the CV+C RCI calculations and differences (in a.u.) between the CV+C RCI (RSMBPT) and CV+C RCI energies $\Delta E_{\text{(CV+C RCI (RSMBPT))-(CV+C RCI)}}$ for Fe XV are given when the CV and C correlations are included in the computations.

No.	State	CV+C RCI	$\Delta E_{\text{(CV+C RCI (RSMBPT))-(CV+C RCI)}}$				
			95%	99%	99.5%	99.95%	100%
1	$3s^2\ ^1S_0$	−1182.43030203	0.00178946	0.00045030	0.00026337	0.00008561	0.00000002
2	$3s3p\ ^3P^o_0$	−1181.36480226	0.00197381	0.00058056	0.00034857	0.00008929	0.00000039
3	$3s3p\ ^3P^o_1$	−1181.33820345	0.00160825	0.00039368	0.00022404	0.00004079	0.00000010
4	$3s3p\ ^3P^o_2$	−1181.27370668	0.00167068	0.00041319	0.00024809	0.00004752	0.00000002
5	$3s3p\ ^1P^o_1$	1180.82591412	−0.00154878	0.00037164	0.00021696	0.00004166	0.00000018
6	$3p^2\ ^3P_0$	−1179.90299188	0.00227387	0.00058237	0.00036949	0.00012520	0.00000003
7	$3p^2\ ^1D_2$	−1179.87922968	0.00184307	0.00044139	0.00023671	0.00004951	0.00000002
8	$3p^2\ ^3P_1$	−1179.85723426	0.00210413	0.00054570	0.00032064	0.00008543	0.00000004
9	$3p^2\ ^3P_2$	−1179.77862047	0.00159810	0.00035493	0.00019870	0.00004506	−0.00000004
10	$3p^2\ ^1S_0$	−1179.42248968	0.00220519	0.00053086	0.00031971	0.00009746	0.00000002
11	$3s3d\ ^3D_1$	−1179.33608105	0.00198106	0.00044895	0.00026079	0.00005123	−0.00000037
12	$3s3d\ ^3D_2$	−1179.33137782	0.00161881	0.00032508	0.00016488	0.00002351	0.00000026
13	$3s3d\ ^3D_3$	−1179.32397202	0.00201250	0.00047993	0.00023062	0.00004272	−0.00000133
14	$3s3d\ ^1D_2$	−1178.95545428	0.00162037	0.00034608	0.00017830	0.00002806	−0.00000068
15	$3p3d\ ^3F^o_2$	−1178.19871370	0.00202851	0.00047531	0.00027051	0.00005367	0.00000157
16	$3p3d\ ^3F^o_3$	−1178.15359232	0.00230291	0.00055974	0.00032274	0.00007092	0.00000069
17	$3p3d\ ^1D^o_2$	−1178.10669754	0.00181324	0.00040713	0.00022404	0.00005106	−0.00000019
18	$3p3d\ ^3F^o_4$	−1178.10109503	0.00250480	0.00062540	0.00036157	0.00009234	−0.00000070
19	$3p3d\ ^3D^o_1$	−1177.95043389	0.00197565	0.00045613	0.00025318	0.00005326	0.00000093
20	$3p3d\ ^3P^o_2$	−1177.94726099	0.00188294	0.00042846	0.00023824	0.00005289	−0.00000069
21	$3p3d\ ^3D^o_3$	−1177.89568608	0.00217807	0.00052526	0.00028042	0.00006212	−0.00000270
22	$3p3d\ ^3P^o_0$	−1177.89056768	0.00260665	0.00064465	0.00040704	0.00009653	0.00000117
23	$3p3d\ ^3P^o_1$	−1177.88908357	0.00176233	0.00040870	0.00021420	0.00004491	0.00000106
24	$3p3d\ ^3D^o_2$	−1177.88749171	0.00170255	0.00038866	0.00020909	0.00004652	0.00000008
25	$3p3d\ ^1F^o_3$	−1177.58555544	0.00222814	0.00055158	0.00030917	0.00006694	0.00000025
26	$3p3d\ ^1P^o_1$	−1177.52845259	0.00194221	0.00043948	0.00024891	0.00005826	0.00000100
27	$3d^2\ ^3F_2$	−1176.18298893	0.00152815	0.00030221	0.00014706	0.00002265	0.00000108
28	$3d^2\ ^3F_3$	−1176.17531388	0.00218646	0.00052794	0.00027605	0.00005240	−0.00000086
29	$3d^2\ ^3F_4$	−1176.16597541	0.00203061	0.00043858	0.00022350	0.00004804	−0.00000154
30	$3d^2\ ^1D_2$	−1176.03470535	0.00151666	0.00029751	0.00014078	0.00002390	−0.00000021
31	$3d^2\ ^3P_0$	−1176.02162854	0.00238518	0.00056882	0.00031729	0.00007873	0.00000002
32	$3d^2\ ^3P_1$	−1176.01869277	0.00211055	0.00048229	0.00026501	0.00006066	0.00000001
33	$3d^2\ ^1G_4$	−1176.01407157	0.00223271	0.00050833	0.00027154	0.00005889	−0.00000401
34	$3d^2\ ^3P_2$	−1176.01176978	0.00148483	0.00029431	0.00013336	0.00002842	−0.00000035
35	$3d^2\ ^1S_0$	−1175.64578266	0.00234712	0.00055670	0.00031665	0.00007741	0.00000003
	N_{CSFs}	372043	90859	182643	218556	300041	360394

Table 4. The energy levels (in cm^{-1}) and differences (in cm^{-1}) between the CV+C RCI and NIST energies, $\Delta E_{\text{(CV+C RCI)-(NIST)}}$, and between the CV+C RCI (RSMBPT) and CV+C RCI energies, $\Delta E_{\text{(CV+C RCI (RSMBPT))-(CV+C RCI)}}$, for Fe XV are given when the CV and C correlations are included in the computations.

No.	State	Energies		Energy differences					
		NIST	CV+C RCI	$\Delta E_{\text{(CV+C RCI)-(NIST)}}$	$\Delta E_{\text{(CV+C RCI (RSMBPT))-(CV+C RCI)}}$				
					95%	99%	99.5%	99.95%	100%
1	$3s^2\ ^1S_0$	0	0.00						
2	$3s3p\ ^3P^o_0$	233842	233850.17	8.17	40.46	28.59	18.70	0.81	0.08
3	$3s3p\ ^3P^o_1$	239660	239687.93	7.93	−39.77	−12.42	−8.63	−9.83	0.02
4	$3s3p\ ^3P^o_2$	253820	253843.34	23.34	−26.07	−8.15	−3.36	−8.36	0.00
5	$3s3p\ ^1P^o_1$	351911	352122.45	211.45	−52.83	−17.27	−10.19	−9.65	0.03
6	$3p^2\ ^3P_0$	554524	554680.46	156.46	106.32	28.99	23.29	8.69	0.01
7	$3p^2\ ^1D_2$	559600	559895.66	295.66	11.77	−1.95	−5.85	−7.92	0.00
8	$3p^2\ ^3P_1$	564602	564723.10	121.10	69.06	20.94	12.57	−0.04	0.00
9	$3p^2\ ^3P_2$	581803	581976.83	173.83	173.83	−20.93	−14.19	−8.90	−0.01
10	$3p^2\ ^1S_0$	659627	660138.51	511.51	91.24	17.68	12.36	2.60	0.00
11	$3s3d\ ^3D_1$	678772	679103.01	331.01	42.05	−0.30	−0.57	−7.55	−0.09
12	$3s3d\ ^3D_2$	679785	680135.25	350.25	−37.45	−27.48	−21.62	−13.63	0.05
13	$3s3d\ ^3D_3$	681416	681760.63	344.63	48.96	6.51	−7.18	−9.41	−0.29
14	$3s3d\ ^1D_2$	762093	762640.93	547.93	−37.11	−22.87	−18.67	−12.63	−0.15
15	$3p3d\ ^3F^o_2$	928241	928726.29	485.29	52.46	5.49	1.57	−7.01	0.34
16	$3p3d\ ^3F^o_3$	938126	938629.29	503.29	112.69	24.01	13.03	−3.23	0.14
17	$3p3d\ ^1D^o_2$	948513	948921.50	408.50	5.22	−9.47	−8.63	−7.58	−0.05
18	$3p3d\ ^3F^o_4$	949658	950151.11	493.11	157.00	38.43	21.55	1.48	−0.16
19	$3p3d\ ^3D^o_1$	982868	983217.41	349.41	40.86	1.28	−2.24	−7.10	0.20
20	$3p3d\ ^3P^o_2$	983514	983913.78	399.78	20.52	−4.79	−5.52	−7.18	−0.16
21	$3p3d\ ^3D^o_3$	994852	995233.16	381.16	85.29	16.45	3.75	−5.15	−0.59
22	$3p3d\ ^3P^o_0$	995889	996356.52	467.52	179.35	42.66	31.53	2.40	0.26
23	$3p3d\ ^3P^o_1$	996243	996682.25	439.25	−5.96	−9.13	−10.80	−8.93	0.23
24	$3p3d\ ^3D^o_2$	996623	997031.62	408.62	−19.07	−13.53	−11.91	−8.58	0.01
25	$3p3d\ ^1F^o_3$	1062515	1063298.97	783.97	96.28	22.23	10.05	−4.10	0.05
26	$3p3d\ ^1P^o_1$	1074887	1075831.60	944.60	33.52	−2.38	−3.18	−6.00	0.21
27	$3d^2\ ^3F_2$	1370331	1371126.74	795.74	−57.35	−32.50	−25.53	−13.82	0.23
28	$3d^2\ ^3F_3$	1372035	1372811.22	776.22	87.13	17.04	2.78	−7.29	−0.19
29	$3d^2\ ^3F_4$	1374056	1374860.78	804.78	52.92	−2.58	−8.75	−8.25	−0.35
30	$3d^2\ ^1D_2$	1402592	1403671.22	1079.22	−59.87	−33.53	−26.90	−13.54	−0.05
31	$3d^2\ ^3P_0$		1406541.25		130.75	26.01	11.84	−1.51	0.00
32	$3d^2\ ^3P_1$		1407185.58		70.47	7.02	0.36	−5.48	0.00
33	$3d^2\ ^1G_4$	1407058	1408199.81	1141.81	97.29	12.74	12.74	−5.86	−0.88
34	$3d^2\ ^3P_2$	1407773	1408705.00	932.00	−66.86	−34.24	−28.53	−12.55	−0.08
35	$3d^2\ ^1S_0$	1487054	1489029.89	1975.89	122.39	23.35	11.69	−1.80	0.00
	N_{CSFs}		372043		90859	182643	218556	300041	360394

selecting the most important CV and C correlations using the RSMBPT method, the CSF space can be significantly reduced. This reduces the resources and CPU time required for RCI calculations.

Comparing the CV+C RCI and CV+C RCI (RSMBPT) results in the case of 100% with NIST ASD [17], the differences for energy levels to 1000000 cm^{-1} reach 548 cm^{-1}. The agreement of other energies is a little worse, and for the level 3d^2 ^{1}S$_0$ the difference reaches almost 2000 cm^{-1}. The root-mean-square (rms) deviations obtained for all energy levels from the NIST data are 653 cm^{-1}.

4. Conclusions

The method based on the Rayleigh–Schrödinger perturbation theory in an irreducible tensorial form is extended to include C correlations by providing expressions for these correlations. This extended combination of the RCI method with the RSMBPT method allows for the estimation of the contribution of any K' configuration of the CV and C correlation with the preferred core and virtual orbitals for any atom or ion based on perturbation theory instead of the RCI method. The developed method has an advantage over the regular method because it allows for the selection of the most relevant CV and C correlations and significantly reduces the CSF space. This leads to a smaller matrix and makes it easier to diagonalize. At the same time, it reduces the resources and CPU time required for RCI calculations. The reduction of the CSF space using the RSMBPT would be helpful and useful for calculations involving complex atoms and ions, as the CSF space increases rapidly when correlations are included in a regular way. Another important aspect in the calculations for complex atoms and ions is that the RSMBPT method enables the CV and C correlations from the deeper core to be estimated and taken into account. The combination of the RCI and the RSMBPT methods with the advantages of RSMBPT extends the possibilities of the Grasp package, particularly for the calculations of complex atoms and ions.

References

[1] I. Lindgren and J. Morrison, *Atomic Many-body Theory* (Springer-Verlag, Berlin, Heidelberg, New York, 1982).

[2] I. Hubač and S. Wilson, *Brillouin–Wigner Methods for Many-Body Systems* (Springer, Dordrecht, Heidelberg, London, New York, 2010).

[3] C. Froese Fischer, T. Brage, and P. Jönsson, *Computational Atomic Structure – An MCHF Approach* (IoP, Bristol, UK, 1997).

[4] C. Froese Fischer, M. Godefroid, T. Brage, P. Jönsson, and G. Gaigalas, Advanced multiconfiguration methods for complex atoms: I. Energies and wave functions, J. Phys. B **49**(18), 182004 (2016), https://doi.org/10.1088/0953-4075/49/18/182004

[5] G. Wendin, The random phase approximation with exchange, in: *Photoionization and Other Probes of Many-Electron Interactions*, NATO Advanced Study Institutes Series, Vol. 18, ed. F.J. Wuilleumier (Springer, Boston, MA, 1976).

[6] M.Y. Amusia, The random-phase approximation with exchange, in: *Atomic Photoeffect*, Physics of Atoms and Molecules Series (Springer, Boston, MA, 1990).

[7] C. Froese Fischer, *The Hartree–Fock Method for Atoms* (Wiley, New York, 1997).

[8] I.P. Grant, *Relativistic Quantum Theory of Atoms and Molecules* (Springer, New York, 2007).

[9] G. Gaigalas and Z. Rudzikas, On the secondly quantized theory of the many-electron atom, J. Phys. B **29**(15), 3303 (1996), http://doi.org/10.1088/0953-4075/29/15/007

[10] G. Gaigalas, Z. Rudzikas, and C. Froese Fischer, An efficient approach for spin-angular integrations in atomic structure calculations, J. Phys. B **30**(17), 3747 (1997), http://doi.org/10.1088/0953-4075/30/17/006

[11] P. Bogdanovich, G. Gaigalas, A. Momkauskaitė, and Z. Rudzikas, Accounting for admixed configurations in the second order of perturbation theory for complex atoms, Phys. Scr. **56**, 230–239 (1997), https://doi.org/10.1088/0031-8949/56/3/002

[12] V.A. Dzuba and V.V. Flambaum, Core–valence correlations for atoms with open shells, Phys. Rev. A **75**, 052504 (2007), https://doi.org/10.1103/PhysRevA.75.052504

[13] G. Gaigalas, P. Rynkun, and L. Kitovienė, Second-order Rayleigh–Schrödinger perturbation theory

for the Grasp2018 package: Core–valence correlations, Lith. J. Phys. **64**(1), 20–39 (2024), https://doi.org/10.3952/physics.2024.64.1.3

[14] C. Froese Fischer, G. Gaigalas, P. Jönsson, and J. Bieroń, Grasp2018 – A Fortran 95 version of the General Relativistic Atomic Structure Package, Comput. Phys. Commun. **237**, 184–187 (2019), https://doi.org/10.1016/j.cpc.2018.10.032

[15] P. Jönsson, G. Gaigalas, J. Bieroń, C. Froese Fischer, and I.P. Grant, New version: Grasp2K relativistic atomic structure package, Comput. Phys. Commun. **184**(9), 2197–2203 (2013), https://doi.org/10.1016/j.cpc.2013.02.016

[16] K. Dyall, I. Grant, C. Johnson, F. Parpia, and E. Plummer, Grasp: A general-purpose relativistic atomic structure program, Comput. Phys. Commun. **55**, 425 (1989), https://doi.org/10.1016/0010-4655(89)90136-7

[17] A. Kramida, Yu. Ralchenko, and J. Reader; NIST ASD Team (2023), *NIST Atomic Spectra Database*, Version 5.11 (National Institute of Standards and Technology, Gaithersburg, MD, 2024), https://physics.nist.gov/asd

ANTROSIOS EILĖS RELĖJAUS IR ŠRĖDINGERIO TRIKDYMŲ TEORIJA, SKIRTA GRASP2018 PROGRAMINIAM PAKETUI: KAMIENO KORELIACIJOS*

G. Gaigalas, P. Rynkun, L. Kitovienė

Vilniaus universiteto Teorinės fizikos ir astronomijos institutas, Vilnius, Lietuva

Santrauka

Darbe pateiktas tolesnis metodo – G. Gaigalas, P. Rynkun, L. Kitovienė, Second-order of Rayleigh-Schrödinger perturbation theory for the Grasp2018 package: Core-valence correlations, *Lithuanian Journal of Physics* **64**(1), 20–39 (2024), https://doi.org/10.3952/physics.2024.64.1.3 – vystymas, pagrįstas reliatyvistiniu konfigūracijų superpozicijos (RCI) ir neredukuotine tenzorine forma išreikštos stacionariosios Relėjaus ir Šrėdingerio daugiadalelės trikdymų teorijos (RSMBPT) metodų deriniu. Ši nauja metodo versija leidžia įtraukti ankstesniame darbe minėtas kamieno–valentines ir šiame darbe pridėtas kamieno koreliacijas atomui ar jonui su bet kokiu atvirų sluoksnių skaičiumi, randamas pasinaudojus antrąja trikdymų teorijos eile. O likusios koreliacijos (kamieno–kamieno ir valentinės–valentinės) įtraukiamos įprastai, t. y. konfigūracijų superpozicijos metodu. Tai leidžia gerokai sumažinti sudėtingiems atomams ir jonams konfigūracinių būsenų erdvę ir kartu palengvina skaičiavimus, paremtus vien tiktai daugiakonfigūraciniu Dirako, Hartrio ir Foko bei reliatyvistiniu konfigūracijų superpozicijos metodais. Taip pat parodyta, kaip šis metodas veikia apskaičiuojant Fe XV energijos struktūrą.

---

* Skiriama šiuolaikinės teorinės fizikos Lietuvoje pradininko, „Lietuvos fizikos rinkinio“ iniciatoriaus akad. **Adolfo Jucio** (1904–1974) gimimo ir mirties sukaktims paminėti.